A New Empirical Nonlinear Model for HEMT and MESFET Devices

Iltcho Angelov, Herbert Zirath, and Niklas Rorsman

Abstract—**A new large signal model for HEMT's and MESFET's, capable of modeling the current-voltage characteristic and its derivatives, including the characteristic transconductance peak, gate-source and gate-drain capacitances is described. Model parameter extraction is straightforward and is demonstrated for different submicron gate-length HEMT devices including different ∂-doped pseudomorphic HEMTs on GaAs and lattice matched to InP, and a commercially available MESFET. Measured and modeled dc and *S*-parameters are compared and found to coincide well.**

Introduction

DIFFERENT empirical models suitable for simulation of GaAs MESFETs in nonlinear circuits have been developed [1]–[6]. Some of the models have been incorporated in commercial Harmonic Balance (HB) simulators. These models are used to predict gain, intermodulation distortion, generation of harmonics, etc, versus bias, for circuits like amplifiers, mixers, and multipliers. Recently, Maas *et al.* [6] pointed out that not only the current-voltage characteristic $I_{ds}[V_{gs}, V_{ds}]$ but also their derivatives have to be modeled correctly, especially if the model is supposed to predict intermodulation distortion. In [6], the $I_{ds}[V_{gs}]$ dependence is modeled as a harmonic series, and the coefficients are fitted to both the measured $I_{ds}[V_{gs}, V_{ds}]$ and its derivatives by using singular-value decomposition. Since the above models are intended mainly to describe the performance of MESFETs, there are increasing demands for general FET models, which model both HEMTs and MESFETs. In particular, the characteristic peak in the transconductance versus gate voltage dependence found in most HEMTs must be correctly modeled. In principle, the model utilized in [2], [6] could be used, but many terms are normally needed and parameter extraction requires special techniques.

We propose a new simple model, where parameter extraction can be made by simple inspection of the experimental $I_{ds}[V_{gs}, V_{ds}]$ and $g_m[V_{gs}]$ dc-characteristics, which models I_{ds} and its derivatives with good accuracy. The model has been applied to FETs based on the following material structures: AlGaAs-GaAs, pseudomorphic (AlGaAs-InGaAs-GaAs) (homogeneously doped and single and double ∂-doped), lattice matched to InP (AlInAs-GaInAs-InP), and GaAs MESFET's with good results.

Manuscript received July 10, 1992; revised July 30, 1992.

The authors are with the Department of Applied Electron Physics, Chalmers University of Technology, S-41296, Göteborg, Sweden.

IEEE Log Number 9203679.

The Model

The drain current function is expressed in accordance with previous models as

$$I_{ds}[V_{gs}, V_{ds}] = I_{dA}[V_{gs}]I_{dB}[V_{ds}] \tag{1}$$

where the first factor is dependent only on the gate voltage and the second only on the drain voltage. The $I_{dB}[V_{ds}]$ term is the same as the one used in other models [1], [4]. For $I_{dA}[V_{gs}]$, however, we propose a function whose first derivative has the same 'bell shaped' structure as the measured transconductance function $g_m[V_{gs}]$. The hyperbolic tangent (tanh) function describes the gate voltage dependencies and its derivatives well and is normally available in commercial HB-simulators i.e.:

$$I_{ds} = I_{pk}(1 + \tanh(\psi))(1 + \lambda V_{ds}) \tanh(\alpha V_{ds}) \tag{2}$$

where I_{pk} is the drain current at which we have maximum transconductance, with the contribution from the output conductance subtracted. λ is the channel length modulation parameter and α is the saturation voltage parameter. The parameters α and λ are the same as those in the Statz and Curtice models. ψ is in general a power series function centered at V_{pk} with V_{gs} as a variable i.e.

$$\psi = P_1(V_{gs} - V_{pk}) + P_2(V_{gs} - V_{pk})^2 + P_3(V_{gs} - V_{pk})^3 + , \tag{3}$$

where V_{pk} is the gate voltage for maximum transconductance g_{mpk}. The selected $I_{ds}[V_{gs}, V_{ds}]$ function has well defined derivatives. An advantage of the selected model is its simplicity. The different parameters can as a first approximation be easily obtained by inspection of the measured $I_{ds}[V_{gs}, V_{ds}]$ at a saturated channel condition as follows: all higher terms in ψ are assumed to be zero, λ is determined from the slope of the I_{ds}–V_{ds} characteristic, I_{pk} and V_{pk} are determined at the peak transconductance g_{mpk}. The intrinsic maximum transconductance g_{mpk} is calculated from the measured maximum transconductance g_{mpkm} by taking into account the feedback effect due to the source resistance, R_s, which can be obtained from dc-measurement [7]:

$$g_{mpk} = \frac{g_{mpkm}}{(1 - R_s g_{mpkm})} \tag{4}$$

P_1 is now obtained as

$$P_1 = \frac{g_{mpk}}{I_{pk}(1 + \lambda V_d)} \approx \frac{g_{mpk}}{I_{pk}}. \quad (5)$$

In some HEMTs, V_{pk} is weakly dependent on the drain voltage V_{ds} in the saturated region. This effect can be accounted for by

$$V_{pk} = V_{pko} + \gamma \cdot V_{ds}. \quad (6)$$

In the non-saturated region and for negative V_{ds}, V_{pk} will vary considerably with V_{ds}, as will be discussed later. The dependence of V_{pk} on V_{ds} must be found (experimentally or modeled) and the model will predict the transistor performance correctly.

The same type of modeling functions were chosen to model the dependencies on gate and drain voltage of capacitances C_{gs} and C_{gd}

$$C[V_{gs}, V_{ds}] = C_A[\tanh(V_{gs})]\, C_B[\tanh(V_{ds})] \quad (7)$$

as suggested in [8], [9]. Due to the similarity of $I_{ds}[V_{gs}, V_{ds}]$ and $C_{gs}[V_{gs}, V_{ds}]$ the functions can be expressed as

$$C_{gs} = C_{gso}[1 + \tanh(\psi_1)][1 + \tanh(\psi_2)] \quad (8)$$

$$C_{gd} = C_{gdo}[1 + \tanh(\psi_3)][1 - \tanh(\psi_4)] \quad (9)$$

where

$$\psi_1 = P_{0gsg} + P_{1gsg}V_{gs} + P_{2gsg}V_{gs}^2 + P_{3gsg}V_{gs}^3 + \cdots \quad (10)$$

$$\psi_2 = P_{0gsd} + P_{1gsd}V_{ds} + P_{2gsd}V_{ds}^2 + P_{3gsd}V_{ds}^3 + \cdots \quad (11)$$

$$\psi_3 = P_{0gdg} + P_{1gdg}V_{gs} + P_{2gdg}V_{gs}^2 + P_{3gdg}V_{gs}^3 + \cdots \quad (12)$$

$$\psi_4 = P_{0gdd} + (P_{1gdd} + P_{1cc}V_{gs})V_{ds} + P_{2gdd}V_{ds}^2 + P_{3gdd}V_{ds}^3 + \cdots. \quad (13)$$

The term $P_{1cc}V_{gs}V_{ds}$ reflects the cross-coupling of V_{gs} and V_{gd} on C_{gd}. When an accuracy on the order of 5–10% of C_{gs} and C_{gd} is sufficient (8)–(13) can be simplified to:

$$C_{gs} = C_{gso}[1 + \tanh(P_{1gsg}V_{gs})][1 + \tanh(P_{1gsd}V_{ds})] \quad (14)$$

$$C_{gd} = C_{gdo}[1 + \tanh(P_{1gdg}V_{gs})] \cdot [1 - \tanh(P_{1gdd}V_{ds} + P_{1cc}V_{gs}V_{ds})]. \quad (15)$$

Equation (15) can be further simplified if cross-coupling at large drain voltages ($V_{ds} > 1$ V) is neglected:

$$C_{gd} = C_{gdo}[1 + \tanh(P_{1gdg}V_{gs})][1 - \tanh(P_{1gdd}V_{ds})]. \quad (16)$$

These equations (14)–(16) are suitable for ∂-doped HEMTs with an undoped AlGaAs spacer-layer, as investigated in this study, since they have a saturated $C_{gs}[V_{gs}]$ characteristic for increasing V_{gs} due to the absence of parasitic MESFET channel formation in the AlGaAs layer, found in HEMTs with a doped AlGaAs layer.

Experimental Verification

The model parameters were extracted for a commercially available MESFET and different submicron gate-length devices, including different ∂-doped pseudomorphic HEMTs on GaAs and lattice matched to InP (Fig. 1), with mushroom gates of length from 0.15 μm to 0.35 μm and gate width from 50 μm to 200 μm, fabricated in our laboratory at Chalmers University. f_T and f_{max} were 70–110 GHz and 120–200 GHz respectively for the short gate-length devices.

DC-parameters were measured by using a HP 4145B parameter analyser. In Figs. 2–5, the result of the measured (V_{ds} = 2 V) and the modeled dc parameters of the different transistors is shown. For most devices, the function ψ, extracted from the measured drain current I_{ds}, is almost a straight line and it is possible to use only the first term in ψ to model the transistor (Figs. 2, 3, 4). For some of them (Fig. 5) it is necessary to use more terms to improve the fitting.

In Fig. 6(a), the measured variation of V_{pk} for one transistor (PM3) with a gate width, L_w, of 2 × 25 μm is shown. At low and at negative values of V_{ds}, V_{pk} varies strongly with V_{ds}. Therefore, the V_{pk} dependence also has to be modeled if the operating conditions of the device correspond to these cases. In the same figure, the modeled V_{pk} is plotted using different approximating functions for the V_{pk} dependence. In Fig. 6(b) and (c), the measured and modeled I_{ds} and g_m versus V_{gs} are presented.

The *S*-parameters were measured by Cascade probes WPH-405 connected to a Wiltron 360 Vector Network Analyzer in the frequency range 0.5–62.5 GHz. Here we present results of measurements of the HEMT (PM2) with the gate width of 200 μm and gate length 0.35 μm for which the influence of fringing and pad capacitances is of less importance compared to the short gate width devices. *S*-parameters were measured at the following bias points for parameter extraction: V_{ds} = −1 V, −0.5 V, 0 V, 0.75 V, 2 V, 3 V and V_g = −1.5 V to +0.5 V with a step of 0.25 V. The parasitic parameters of the transistor (Fig. 7(a)) can be found most accurately at V_{ds} = 0. This regime is also important for mixers working in the resistive mode [10]. At V_{ds} = 0.75 V, I_{ds} is saturated. At V_{ds} = 2–3 V the transistor is working in its normal operating mode.

The intrinsic parameters of the equivalent circuit (Fig. 7(a)) were derived. The parasitic parameters L_g, L_d, L_s, R_g, R_d, C_p were fixed at the parameter values extracted from the *S*-parameter measurement at V_{ds} = 0.

Our model was easily implemented in a commercial Harmonic Balance-simulator (MDS from HP) as a custom defined equation model. The model parameters of the PM2 (L_w = 200 μm, L_g = 0.35 μm) HEMT are listed in Table I. For this particular HEMT we have to include the cubic

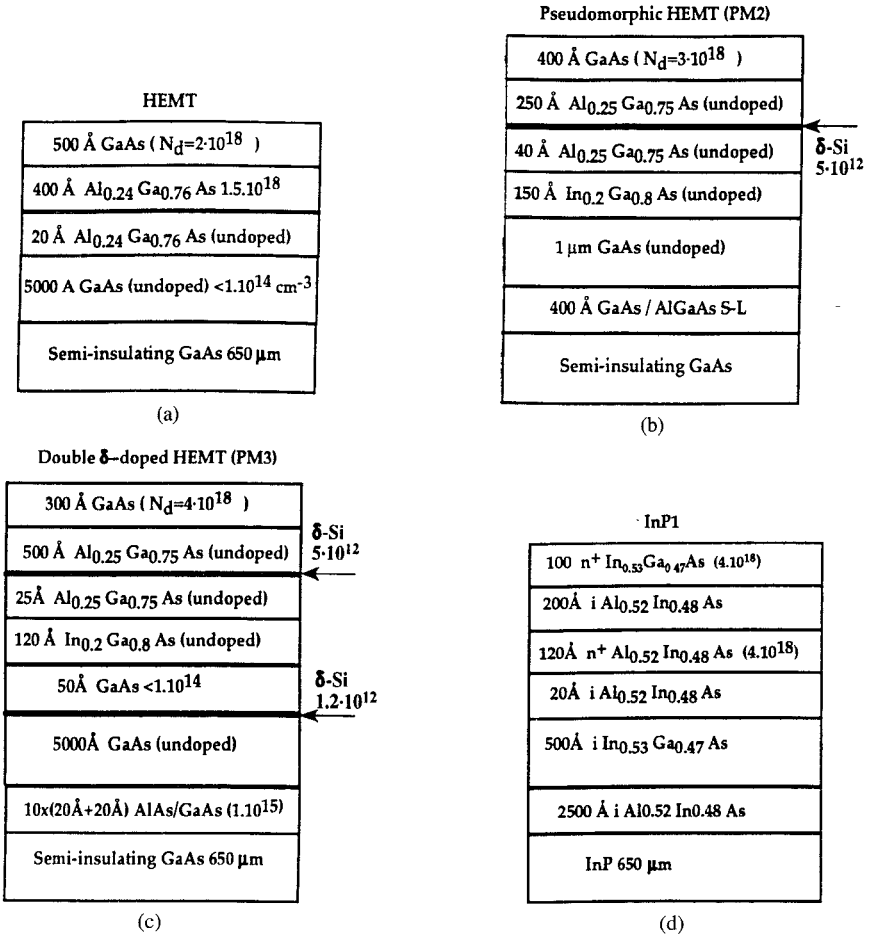

Fig. 1. Structure of the devices. (a) Ordinary HEMT. (b) Pseudomorphic HEMT (PM2). (c) Double δ-doped pseudomorphic HEMT (PM3). (d) Lattice matched to InP HEMT.

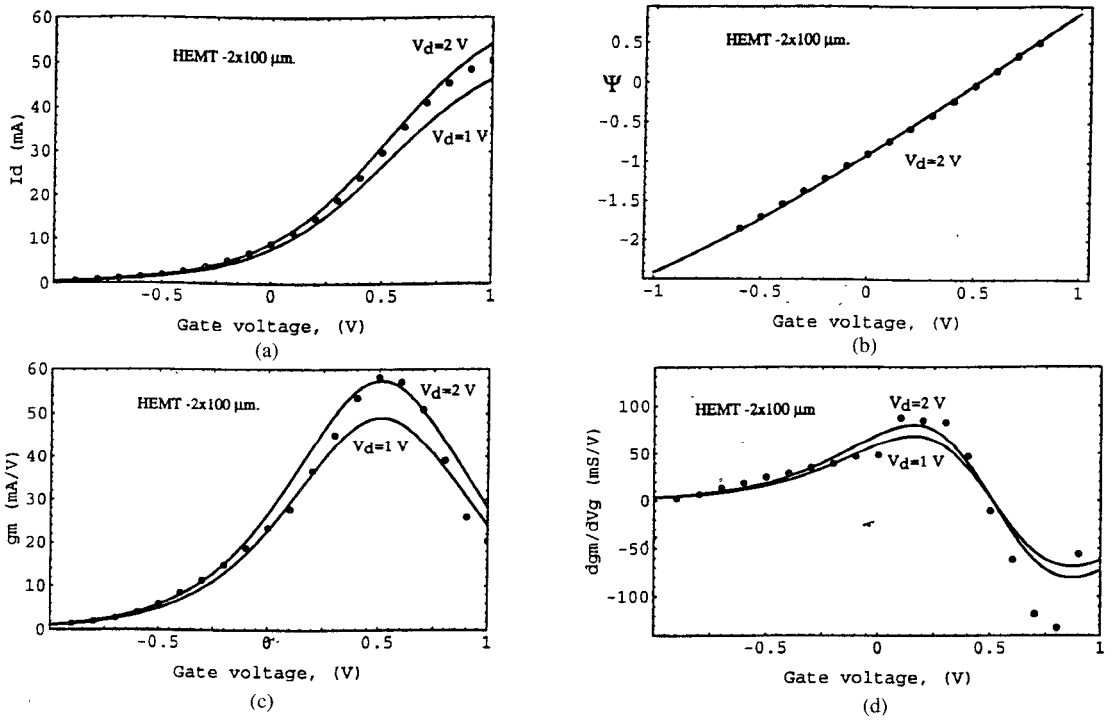

Fig. 2. Measured V_d = 2 V (dots) and modeled (solid lines) characteristic of ordinary HEMT (L_w = 2 × 100 µm, L_g = 0.15 µm). (a) Drain current I_{ds}, versus gate voltage, V_{gs} (I_{pk} = 31 mA, λ = 0.02, α = 1.3, V_{pk} = 0.51 V). (b) ψ-function versus gate voltage, V_{gs} (P_1 = 1.8, P_2 = 0, P_3 = −0.09). (c) Transconductance, g_m, versus gate voltage, V_{gs}. (d) Derivative of the transconductance $d(g_m)/dV_{gs}$.

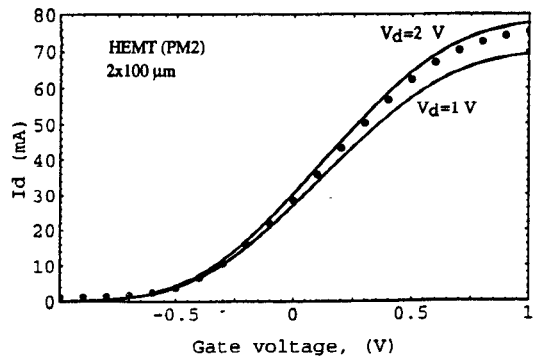

(a)

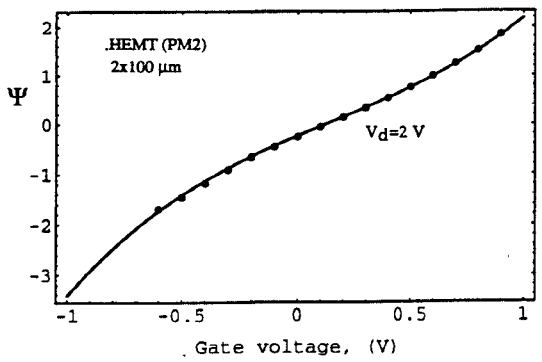

(b)

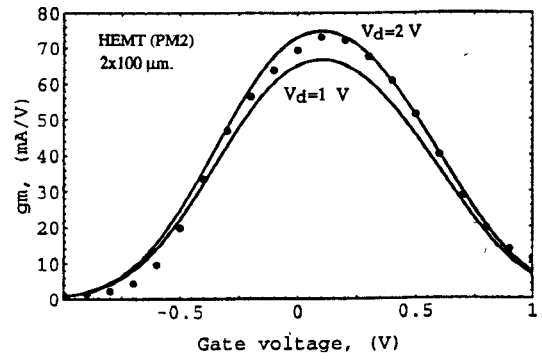

(c)

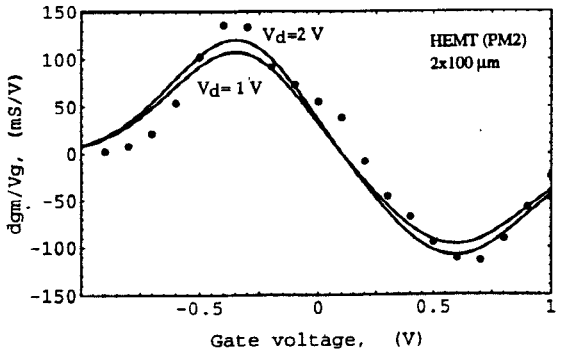

(d)

Fig. 3. Measured V_d = 2 V (dots) and modeled (solid lines) characteristics of pseudomorphic HEMT (PM2) (L_w = 2 × 100 μm, L_g = 0.15 μm). (a) Drain current, I_{ds}, versus gate voltage, V_{gs} (I_{pk} = 38 mA, λ = 0.02, α = 1.5, V_{pk} = 0.12 V). (b) ψ-function versus gate voltage, V_{gs} (P_1 = 1.9, P_2 = 0, P_3 = 0.83). (c) Transconductance, g_m, gate voltage, V_{gs}. (d) Derivative of the transconductance $d(g_m)/dV_{gs}$.

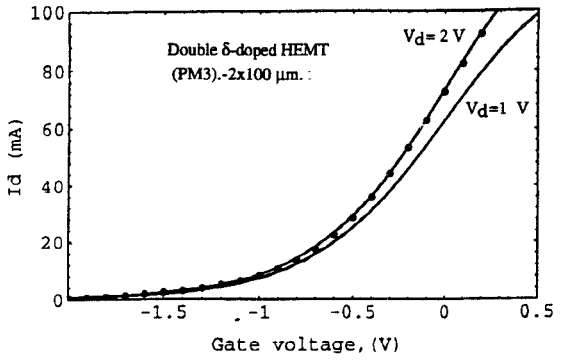

(a)

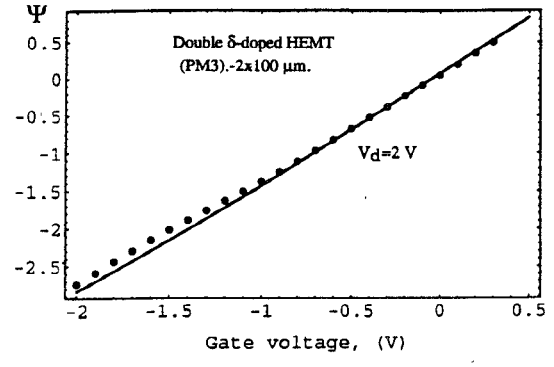

(b)

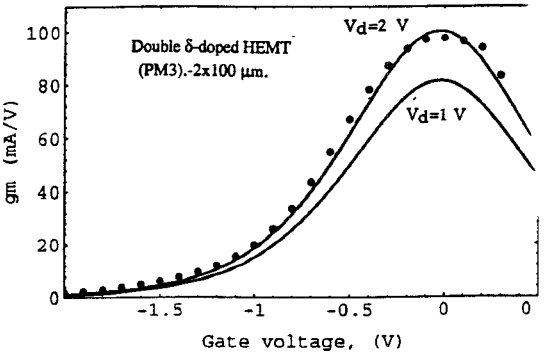

(c)

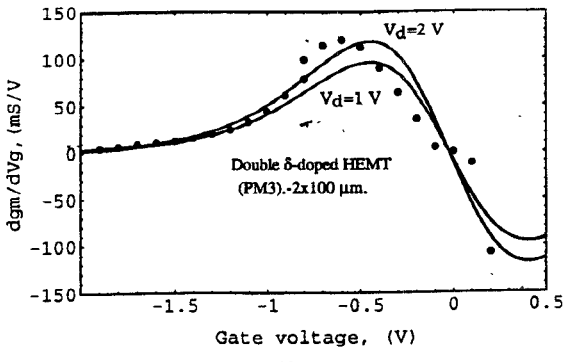

(d)

Fig. 4. Measured V_d = 2 V (dots) and modeled (solid lines) characteristics of double δ-doped HEMT (PM3) (L_w = 2 × 100 μm, L_g = 0.15 μm). (a) Drain current, I_{ds}, versus gate voltage, V_{gs} (I_{pk} = 69 mA, λ = 0.025, α = 1.3, V_{pk} = −0.0.25 V). (b) ψ-function versus gate voltage (P_1 = 1.42, P_2 = 0, P_3 = −0.02). (c) Transconductance, g_m, versus gate voltage, V_{gs}. (d) Derivative of the transconductanee $d(g_m)/dV_{gs}$.

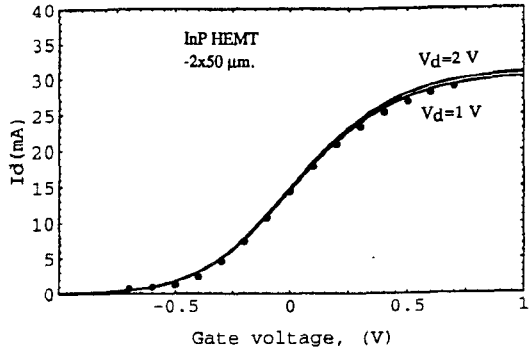

(a)

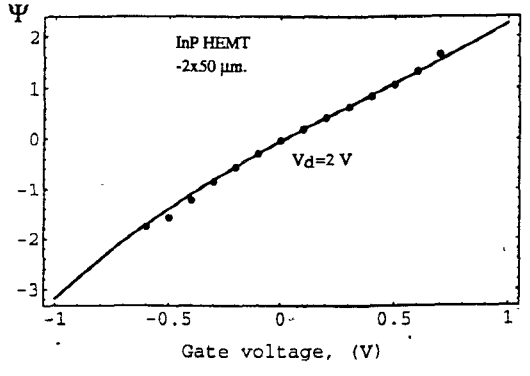

(b)

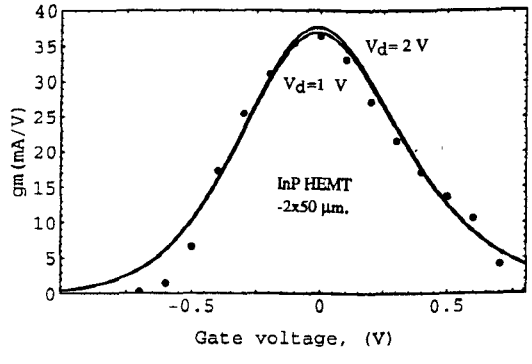

(c)

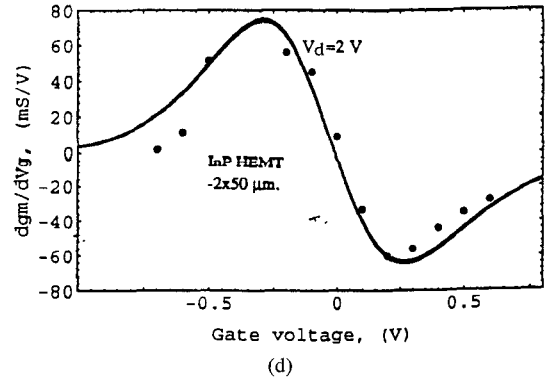

(d)

Fig. 5. Measured $V_d = 2$ V (dots) and modeled (solid lines) characteristics of InP-HEMT ($L_w = 2 \times 50$ µm, $L_g = 0.15$ µm). (a) Drain current, I_{ds}, versus gate voltage, V_{gs} ($I_{pk} = 15$ mA, $\lambda = 0.02$, $\alpha = 1.5$, $V_{pk} = 0.02$ V). (b) ψ-function versus gate voltage, V_{gs} ($P_1 = 2.4$, $P_2 = -0.4$, $P_3 = 0.02$ V). (c) Transconductance, g_m, versus gate voltage, V_{gs}. (d) Derivative of the transconductance $d(g_m)/dV_{gs}$.

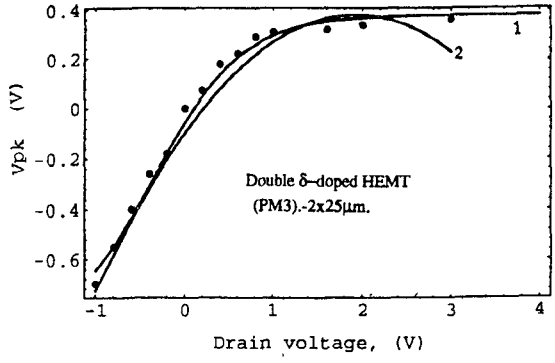

(a)

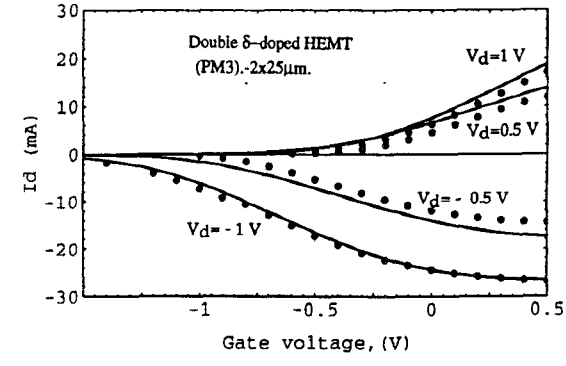

(b)

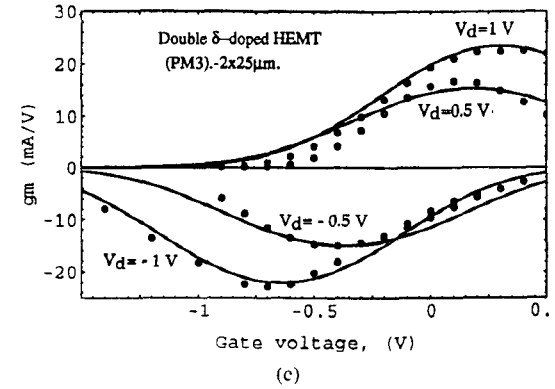

(c)

Fig. 6. Measured (dots) and modeled (solid lines) characteristics of double δ-doped HEMT (PM3) ($L_w = 2 \times 25$ µm, $L_g = 0.15$ µm). (a) V_{peak} versus V_{ds}: 1) $V_{pk} = -0.27 + 0.65(\text{Tanh}[(V_{ds} + 0.34)]$ and 2) $V_{pk} = -0.1 + 0.5\ V_{ds} - 0.13V_{ds}^2$. (b) Drain current, I_{ds}, versus gate voltage, V_{gs} ($I_{pk} = 16$ mA, $\lambda = 0.03$, $\alpha = 1.3$, $P_1 = 1.65$, $P_2 = 0$, $P_3 = 0.5$, $V_{pk} = -0.27 + 0.65(\text{Tanh}[(V_{ds} + 0.34)])$. (c) Transconductance, g_m, versus gate voltage, V_{gs}.

term in order to improve the fitting of the drain current and its derivates at voltages close to pinch-off. All terms except P_1 and P_3 are zero.

In Fig. 7(b)–(d), the measured and modeled I_{ds}–V_{ds} characteristics, the transconductance g_m, and the output resistance, R_{ds}, are plotted, respectively.

Fig. 8 shows the measured and simulated S-parameters of the transistor at different bias points. The difference between the modeled and simulated values is small for all S-parameters. The model has been also used to simulate the performance of different non-linear circuits like mixers and multipliers with good accuracy [12], [13].

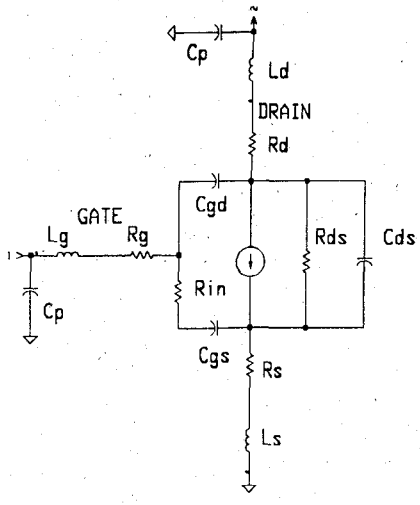

(a)

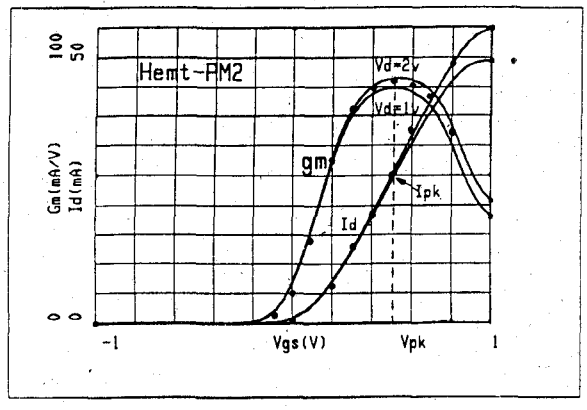

(c)

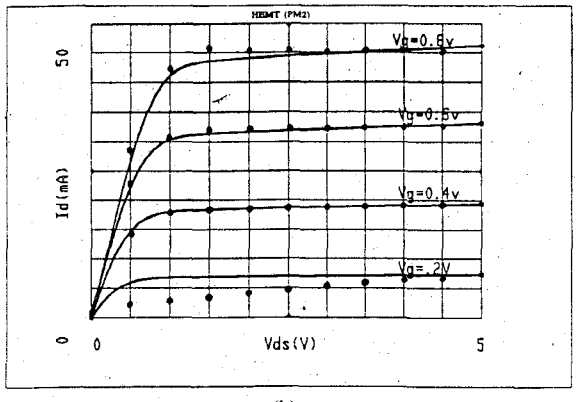

(b)

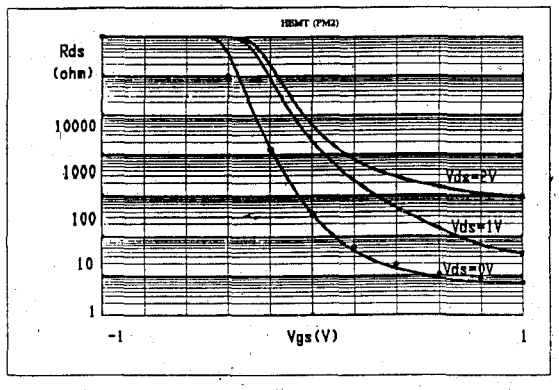

(d)

Fig. 7. Measured (dots) and modeled (solid lines) PM2 HEMT characteristics (L_w = 200 μm, L_g = 0.35 μm). (a) The equivalent circuit of the transistor. (b) Drain current, I_{ds}, versus drain voltage, V_{ds}. (c) Drain current, I_{ds}, and transconductance, g_m, versus gate voltage, V_{gs}. (d) Drain-source resistance, R_{ds}, gate voltage, V_{gs}.

TABLE I
EXTRACTED PARAMETERS OF THE HEMT

R_g [Ω]	R_{gs} [Ω]	R_s [Ω]	R_d [Ω]	C_{ds} [Ω]	C_{gs} [pF]	C_{gd} [fF]
3	3.5	3	6	60	0.28	35
I_{pk} [mA]		P_1	P_3	V_{pk} [V]	λ	α
26.3		3.35	7	0.55	0.02	3

Figs. 9(a)–(c) show the measured and modeled dependencies of C_{gs} and C_{gd} for transistors with gate dimensions of 200 μm × 0.35 μm. The commonly used models (pn-junction or Statz models) are not appropriate for this case. For the studied pulse-doped pseudomorphic HEMT the following simple expressions were found (with simple curve fitting procedure [11]) giving an accuracy, which is sufficient for most practical cases:

$$C_{gs} = C_{gso}[1 + \tanh(V_{gs} - 0.048V_{gs}^2)] \cdot [1 + \tanh(0.4V_{ds})] \quad (17)$$

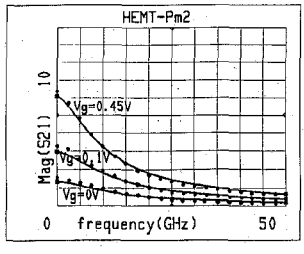

(a)

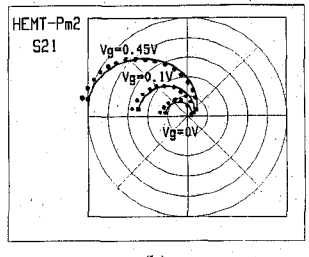

(b)

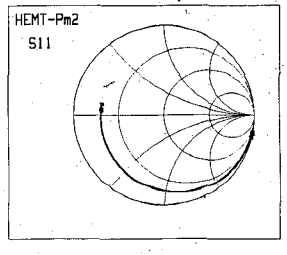

(c)

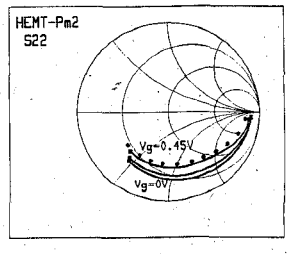

(d)

Fig. 8. The measured (dots) and modeled (solid lines) S-parameters of the PM2 HEMT (L_w = 200 μm L_g = 0.35 μm) for V_{ds} = 2 V and V_{gs} = 0 V, 0.1 V and 0.45 V. (a) Magnitude of S_{21}. (b) S_{21}. (c) S_{11}. (d) S_{22}.

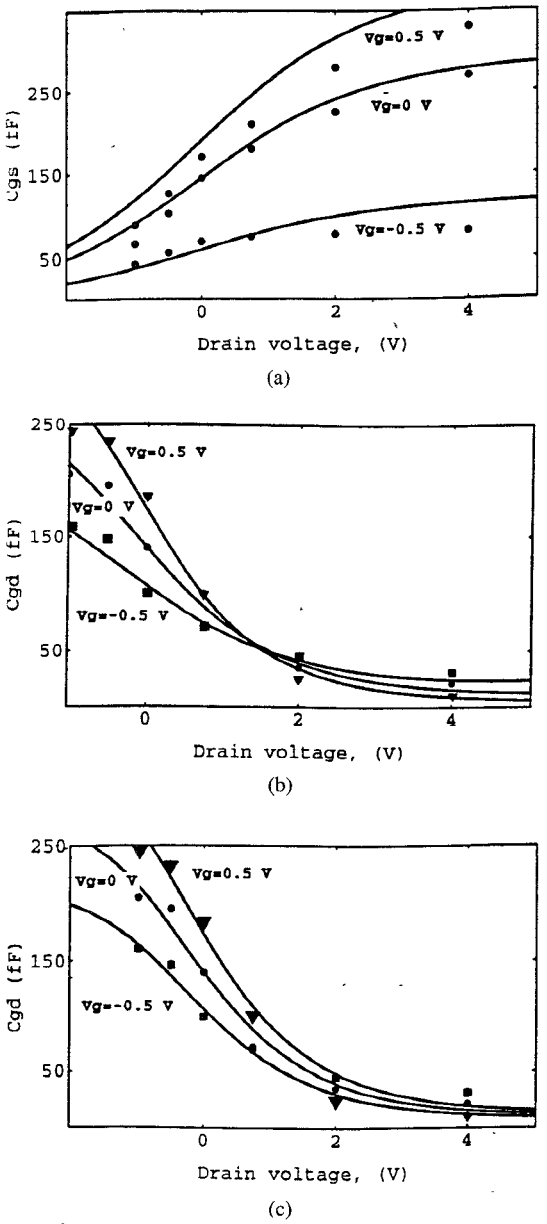

Fig. 9. Measured (dots) and modeled (solid lines) capacitances of the PM2 HEMT (L_w = 200 μm, L_g = 0.35 μm) (C_{gso} = C_{gdo} = 145 fF). (a) C_{gs} versus V_{ds} eq. (17). (b) C_{gd} versus V_{ds} eq. (18). (c) C_{gd} versus V_{ds} eq. (19).

$$C_{gd} = C_{gdo}[1 + \tanh(0.48V_{gs})] \cdot [1 - \tanh(0.55V_{ds} - 0.048V_{ds}^2 + 0.2V_{gs}V_{ds})] \quad (18)$$

and for the simplified equation of C_{gd} we obtain:

$$C_{gd} = C_{gdo}[1 + \tanh(0.48V_{gs})][1 - \tanh(0.55V_{ds})] \quad (19)$$

where $C_{gso} = C_{gdo}$ = 145 fF are the capacitances for $V_{gs} = V_{ds} = 0$.

In Fig. 9(b) and (c), the modeled C_{gd} using (18) and (19) are shown. Evidently even such a simple equation as (19) gives good accuracy. When higher accuracy is required more terms should be included.

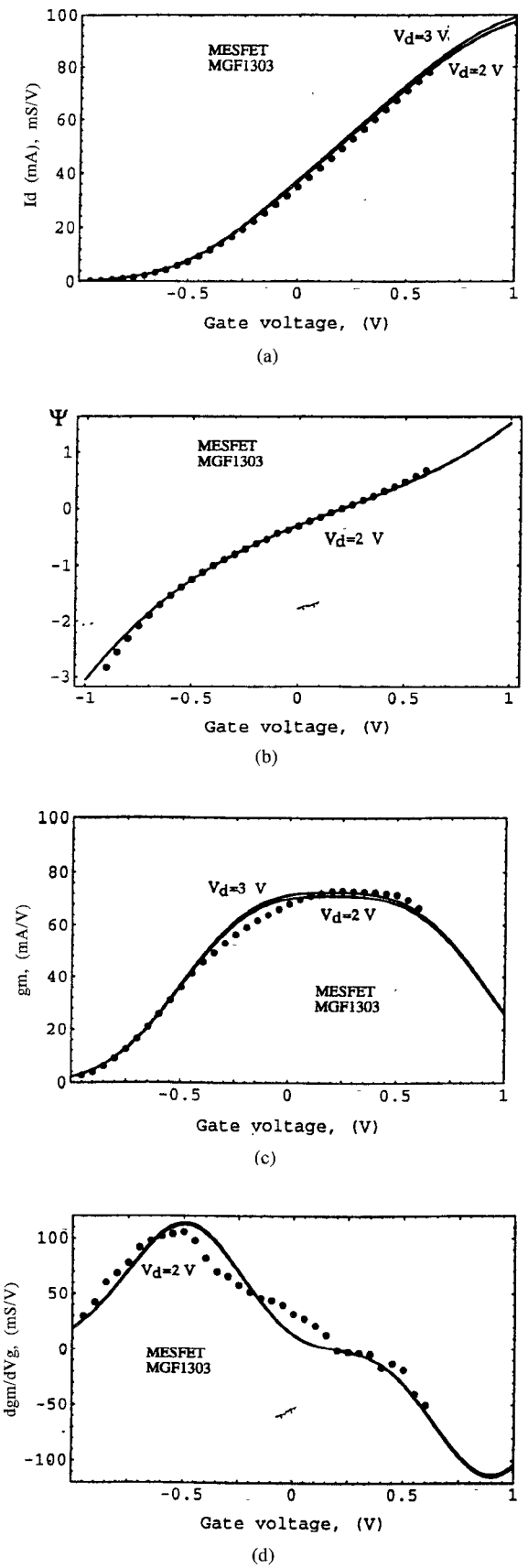

Fig. 10. Measured (dots) and modeled (solid lines) MESFET (MGF1303) characteristics. (a) Drain current, I_{ds}, versus gate voltage, V_{gs} (I_{pk} = 49 mA, λ = 0.02, α = 3). (b) ψ-function versus gate voltage, V_{gs} (P_1 = 1.4, P_2 = 0, P_3 = 0.8, V_{pk} = 0.2 V). (c) Transconductance, g_m, versus gate voltage, V_{gs}. (d) Derivative of the transconductance $d(g_m)/dV_{gs}$.

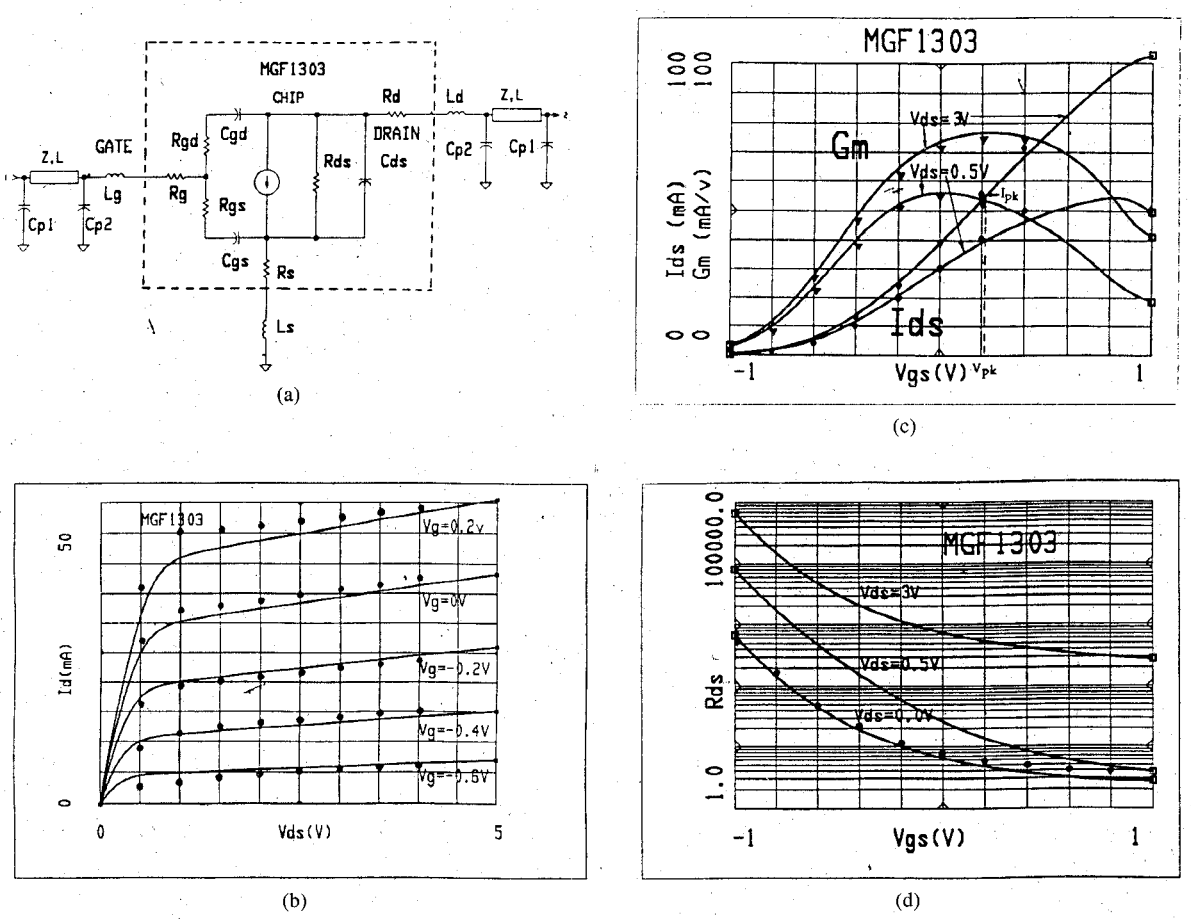

Fig. 11. Measured (dots) and modeled (solid lines) MESFET (MGF1303) characteristics. (a) The equivalent circuit of the packaged transistor. (b) Drain current, I_{ds}, versus drain voltage, V_{ds}. (c) Transconductance, g_m, versus gate voltage, V_{gs}. (d) Drain-source resistance, R_{ds}, versus gate voltage, V_{gs}.

TABLE II
EXTRACTED PARAMETERS OF THE MESFET MGF1303

R_g [Ω]	R_{gs} [Ω]	R_s [Ω]	R_d [Ω]	R_c [Ω]	R_{gd} [Ω]	C_{ds} [fF]	C_{rf} [pF]	C_{gs} [pF]	C_{gd} [fF]	C_{p1} [fF]	C_{p2} [fF]	Z [Ω]	L [mm]
2.4	2.2	3.7	3.3	750	30	130	0.35	0.52	45	32	200	80	0.45

I_{pk} [mA]	P_1	P_3	V_{pk} [V]	λ	α	L_g [nH]	L_d [nH]	L_s [nH]
49.3	1.5	0.7	0.2	0.04	3.5	0.38	0.3	0.05

The same study was performed on an ordinary MESFET and the model was shown to work equally well for this kind of device. Model parameters were extracted for packaged MESFETs fabricated by different manufactures. DC- and *S*-parameters were measured using a Maury MT-950 transistor fixture and Wiltron 360/HP 8510 C ANA in the frequency range 0.1–18 GHz.

The measured and simulated dc parameters of the Mitsubishi MGF 1303, the drain current, I_{ds}, the ψ-function, the transconductance, g_m, the derivative of the transconductance, g_m, are shown in Fig. 10. We have used a more complicated equivalent circuit of the transistor (Fig. 11(a)) to model the packaged transistors accurately. Parameters were extracted in the same way as for the HEMT as described above. The model parameters listed in Table II extracted for a MESFET (MGF 1303), were used in Harmonic Balance Simulator (MDS) to simulate the dc and microwave performance of this transistors.

In Fig. 11(b)–(d) the measured and modeled I_{ds}–V_{ds} dependence, the transconductance, g_m, versus gate voltage V_{gs}, the output resistance, R_{ds}, for this packaged transistor are shown. Measured and simulated *S*-parameters for the MESFET at different bias conditions are shown in Fig. 12. The difference between measured and modeled I_{ds} versus V_{gs}, g_m and S_{21} is less than 5%.

CONCLUSIONS

A practical, simple, and accurate large-signal empirical model capable of modeling the drain current-gate voltage characteristic and its derivatives, and the capacitances C_{gs}

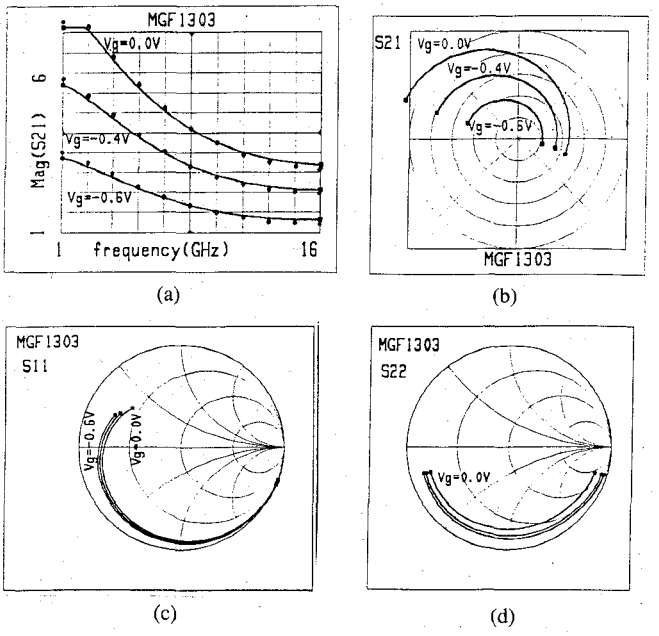

Fig. 12. The measured (dots) and simulated (solid lines) S-parameters of the MESFET (MGF1303) (V_{ds} = 3 V; V_{gs} = 0 V, −0.45 V, −0.6 V). (a) Magnitude of S_{21}. (b) S_{21}. (c) S_{11}. (d) S_{22}.

and C_{gd} for HEMTs and MESFETs is presented. Parameter extraction and the incorporation of this model into commercial software tool is straightforward. The model has been used to predict the dc- and S-parameters of the devices and to simulate the performance of different nonlinear circuits like mixers and multipliers with good accuracy.

Acknowledgment

The authors would like to thank C. Kärnfelt at Ericsson Radar Electronics (ERE) for help with the substrates and bonding, and T. Andersson at Chalmers University of Technology for fabricating the test fixtures, and C. Karlsson for help with the fabrication of HEMTs. The Swedish Defence Material Administration (FMV) and The Swedish National Board for Industrial and Technical Development (NUTEK) are acknowledged for financial support, QED and NSI for growing MBE heterostructure materials, and Prof. E. Kollberg, Dr. L. Lundgren, Dr. T. Lewin, Dr. R. Weikle and G. Ericsson for their support of this work.

References

[1] W. Curtice, "A MESFET model for use in the design of GaAs integrated circuits," *IEEE Trans. Microwave Theory Tech.*, vol. MTT-28, no. 5, pp. 448–455, 1980.

[2] W. Curtice and M. Ettenberg, "A nonlinear GaAs FET model for use in the design of output circuits for power amplifiers," *IEEE Trans. Microwave Theory Tech.*, vol. MTT-33, no. 12, p. 1383, 1985.

[3] A. Materka and T. Kacprzak, "Computer calculation of large-signal GaAs FET amplifier characteristics," *IEEE Trans. Microwave Theory Tech.*, vol. MTT-33, no. 2, pp. 129–134, 1985.

[4] H. Statz, P. Newman *et al.* "GaAs FET device and circuit simulation in SPICE," *IEEE Trans. Electron Devices*, vol. ED-34, pp. 160–166, 1987.

[5] Y. Tajima, B. Wrona, and K. Mishima, "GaAs FET large-signal model and its application to circuit design," *IEEE Trans. Electron Devices*, vol. 28, p. 171, 1981.

[6] S. Maas and D. Neilson, "Modeling of MESFETs for intermodulation analysis of mixers and amplifiers," in *1990 IEEE MTT-S Microwave Symp. Dig.*, pp. 1291–1294.

[7] R. Holmstrom, W. Bloss, and J. Chi, "A gate probe method of determining parasitic resistance in MESFETs," *IEEE Electron Device Lett.*, vol. 7, pp. 410–412, 1986.

[8] P. Roblin, S. Kang, and H. Morkoc, "Analytic solution of the velocity-saturated MOSFET/MODFET wave equation and its application to the prediction of the microwave characteristics of MODFETs," *IEEE Trans. Electron Devices*, vol. 37, 1990.

[9] D. Arnold, W. Kopp, R. Fisher, J. Klem, and H. Morkoc, "Bias dependence of capacitances in MODFET at 4 GHz," *IEEE Electron Device Lett.*, vol. EDL-5, p. 123, 1984.

[10] S. Maas, "A GaAs MESFET mixer with very low intermodulation," *IEEE Trans. Microwave Theory Tech.*, vol. MTT-35, no. 4, pp. 425–430, 1987.

[11] S. Wolfram, *Mathematica*. Reading, MA: Addison-Wesley, 1991.

[12] I. Angelov, H. Zirath, N. Rorsman, and H. Grönqvist, "A balanced millimeter wave doubler based on pseudomorphic HEMTs," in *1992 IEEE MTT-S Microwave Symp. Dig.*, p. 353–356.

[13] I. Angelov, H. Zirath, N. Rorsman, E. Kollberg, "Characteristics of millimeter wave drain mixer," in *1992 EUMC Rec.*, Helsinki, Finland.

Iltcho Angelov received the M.S. degree in electronics in 1969 and the Ph.D. degree in physics and mathematics in 1973.

He worked with parametric amplifiers, IMPATT and Gunn oscillators, studied nonlinear effects and synchronisation phenomena in these devices. Since 1976 he has worked with microwave low noise transistor amplifiers, including criogenically cooled amplifiers. Recently his research activity is in the field of HEMT nonlinear modelling and development of millimeter wave HEMT mixers and multipliers.

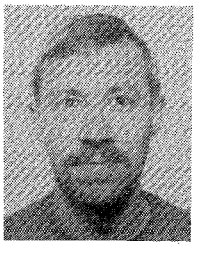

Herbert Zirath received the M.Sc. degree in electrical engineering in 1980 and the Ph.D. degree in 1986 from Chalmers University of Technology, Göteborg, Sweden.

Since 1980, he has been working as a researcher at Chalmers on cooled millimeter-wave Schottky diode mixers and on the properties of millimeter-wave Schottky barrier diodes. In addition, he has been responsible for the development of active millimeter-wave components like MESFET and HEMT including their modeling, and related circuits, like mixers, amplifiers and harmonic generators, since 1986.

Niklas Rorsman received the M.Sc. degree in engineering physics in 1988 and the degree of licentiate of engineering in 1992 from Chalmers University of Technology. He is currently working towards the Ph.D. degree. Since 1988 he has been working with development of heterostructure field effect transistors and their applications.